Asian Journal of Chemistry; Vol. 36, No. 10 (2024), 2311-2317

ASIAN JOURNAL OF CHEMISTRY

https://doi.org/10.14233/ajchem.2024.32331

Fabrication of Chitosan-Cu_2O Nanocomposite through Ethanol Assisted Reduction

E. DILLU*, and S.H. KHAN

Department of Chemistry, Sam Higginbottom University of Agriculture, Technology & Sciences, Prayagraj-211007, India

*Corresponding author: E-mail: elbrightdillu@gmail.com

Received: 19 July 2024; *Accepted*: 23 August 2024; *Published online*: 30 September 2024; AJC-21762

The semiconducting characteristics of copper oxides have intrigued researchers like photocatalysis and sensors. Coating these nanoparticles with biocompatible polymers like chitosan enhances their properties, such as biocompatibility and non-toxicity, while reducing production costs. This work details the successful *in situ* production of a biocompatibile nanocomposite, with Cu_2O nanoparticles dispersed in a chitosan matrix using ethanol as a reducing agent. Advanced techniques including ultraviolet-visible (UV-Vis) spectroscopy, X-ray diffraction (XRD), Fourier transform infrared (FTIR) spectroscopy, scanning electron microscopy (SEM) and transmission electron microscopy (TEM) imaging combined with selected area electron diffraction (SAED) analysis, have been employed to characterize the nanocomposite material with additional relevant properties analyzed.

Keywords: Nanocomposite, Chitosan, Reduction, Biopolymer, Semiconductor nanoparticles.

INTRODUCTION

The synthetic pathway for the preparation of metal and metal oxide nanoparticles has attracted a lot of researchers in recent years, especially because there has been a dire need for a greener approach towards the same [1]. In response to this, several researchers have come up with ideas involving employment of biopolymers as reducing and stabilizing agents for the synthesis of nanoparticles, thus leading to a significant evolution in nanochemistry involving synthesis of varied nanomaterials where nanoparticles are embedded inside the polymer matrix also called nanocomposites. Nanocomposites can be described as materials composed of several components, each having distinct phase domains. In these materials, there is at least one phase where one dimension measures in the nanometer scale [2]. Intriguing possibilities emerge with the versatile applications of metallic copper and copper oxide nanoparticles spanning catalysis, biomedical fields, sensing materials and solar cells [3]. An interesting feature of metal oxide nanoparticles including nanoparticles of copper oxide is their behaviour as semiconductors, which finds use in emerging fields like photocatalysis, sensing, superconduction, photovoltaics, solar cells, lithium ion batteries, medical diagnosis, *etc*. Hence, great attention has been drawn to the exploration of synthetic routes leading to cuprous oxide and cupric oxide nanoparticles. The Cu_2O nanoparticles, especially, have been recognized as p-type semiconductors and their important physical and chemical properties have come under thorough investigation in the current research scenario [4]. Moreover, many researchers have shown that quantum confinement effect of electrons or electron-hole pairs are responsible for the way light interacts with matter; exciton confinement in case of semiconductor nanoparticles is a consequence of that which opens up possibilities of achieving important modifications in properties through band gap engineering in semiconductors [5].

It has been well-known that metal oxide nanoparticles show promising results in several fields including biomedical, also, the preparation procedures are simple in nature, can be tailored easily into desired size and morphology, are highly stable and do not show any variations in swelling and can be combined easily with hydrophilic and hydrophobic systems. In this view, the research for synthesizing new nanomaterials involving nanosized copper oxides has become an interesting field [6]. Furthermore, copper and its complexes have been utilized for sterilization since significantly long time due to their tested antimicrobial properties [7]. Despite this potential being proved to an even greater extent in the nanomaterials involving copper, the inherent toxicity of these nanoparticles limits their use in

biological systems. However, a compelling solution lies in employing biodegradable polymers like polyactic acid, cellulose, starch, alginate, *etc.* which have been extensively studied for their use as a matrix for synthesis and stabilization of nanoparticles. In regards to this, the biocompatible and environmentally safe nature of chitosan, a derivative biopolymer of chitin, has been exploited by several researchers [8,9]. It can be obtained by the deacetylation of chitin using concentrated sodium hydroxide solution, where the amide groups of the biopolymer are converted to amino groups [10]. These amino groups along with the hydroxyl groups found in the biopolymer are responsible for its various properties such as complexation with metal ions leading to their reduction and stabilization as nanosized particles, cell adhesion, which plays a fundamental role in its antibacterial nature and biocompatibility which renders it desirable in biomedical applications [11]. Chitosan not only serves as an ideal matrix for nanoparticle synthesis but also effectively addresses challenges related to nanoparticle growth and oxidation, crucial factors for practical applications [12,13].

Chitosan is a powerful stabilizer that apart from efficiently slowing down the growth-rate of nanoparticle size also prevents copper nanoparticles from easily reacting with oxygen by acting as a physical barrier between atmospheric oxygen and nanoparticles, which is a important factor to take into account since copper nanoparticles are difficult to store even in airtight containers because they easily oxidize when exposed to air [14]. Additionally, chitosan has been found to have antibacterial properties. However, when combined with copper, chitosan and copper nanocomposites exhibit greater antibacterial activities than their pure forms, making them a great choice for antibacterial applications [15]. In addition to improving the biocompatibility of the resulting nanocomposites, biopolymers like chitosan also lower production costs [16]. Chitosan has become a popular choice of support matrix for the stabilization of nanoparticles, consequently. Chitosan's polar functional groups link with the metal ion precursor during the reduction and stabilization processes thereby aiding the formation of nanoparticles. Furthermore, chitosan is a more environmentally friendly option than synthetic polymers used for the same purpose because it is derived from natural sources and is biodegradable [17].

Several synthetic methods have been used to prepare chitosan-copper nanocomposites, using reducing agents like ascorbic acid, hydrazine, sodium borohydride, sodium phosphinate and polydentate ligands, among others [18-22]. An attempt has been made to prepare biocompatible chitosan-cuprous oxide (CS-Cu_2O) nanocomposite through the ethanol-assisted reduction of metal ions. In other contexts, ethanol has been used as a reducing agent to form metal nanoparticles other than copper, which is likely due to the fact that copper nanoparticles are more inclined to oxidation and easily convert to CuO upon exposure to air and hence harsh chemical methods are the preferred options for the synthesis of copper nanoparticles [23,24]. However, ethanol has been deemed as a comparatively environment friendlier alternative for the purpose of reduction and been called as a greener mono-alcohol. It has been substantially argued that ethanol is a better prospect even compared to methanol when it comes to metal ion reduction during nanoparticle synthesis because of its cheap cost and easy availability [25,26].

Thus, this work reports the synthetic procedures carried out for the development of chitosan-cuprous oxide (CS-Cu_2O) nanocomposite and characterized. The UV-visible spectral analysis has been utilized to preliminarily confirm the formation of nanoparticles and shed light on the optical properties of the nanomaterial, including its optical band gap. The interaction of metal with chitosan has been explored through FTIR transmittance data, whereas, the morphological details have been observed and reported with the electron microscopic images. The identification of lattice parameters and the formation of nanoparticles have been discussed through XRD and SAED patterns obtained during HRTEM analysis. The oxidation state of metal has been further confirmed by X-ray photoelectron spectroscopy.

EXPERIMENTAL

Copper sulphate pentahydrate, ethanol, glacial acetic acid, sodium hydroxide and chitin used in this work were purchased from Merck.

Preparation of chitosan solution: High molecular weight chitin was ground to a fine powder and deacetylated using several cycles of heating in 50% NaOH followed by centrifugation till a small sample of the resultant chitosan was found to be soluble in acidic medium. The chitosan so formed was separated from the NaOH solution using centrifugation followed by decantation, washed several times with double distilled water till the decanted liquid showed neutral pH and dissolved in 1% acetic acid solution to obtain a colloidal solution of chitosan [27,28]. Small portions of chitin and chitosan powders were dried in hot air oven at 60 ºC and the dried powder was characterized using Fourier transform infrared (FTIR) spectroscopic analysis.

Preparation of chitosan-Cu_2O (CS-Cu_2O) nanocomposite: A $CuSO_4$ solution (25 mL of 75 mM) was mixed with 50 mL of 1% chitosan solution (in 1% acetic acid) under constant stirring to obtain a light blue solution. Pure ethanol (25 mL) was added, the pH was adjusted to 8 by adding dilute NaOH dropwise and the resultant mixture was agitated at 500 rpm for 30 min in an inert atmosphere, thereby causing a transition from blue to brown colour. The brown colour mixture was centrifuged at 5000 rpm, the obtained precipitate was washed with ethanol, dried at room temperature and analyzed [29,30].

Characterization: For UV-visible spectral analysis, the aqueous dispersion of precipitate was scanned within wavelength range 200 nm to 750 nm using Shimadzu® UV-VIS NIR spectrophotometer, UV-3600 Plus model using quartz cuvettes. The FTIR spectrum was recorded using Perkin-Elmer Spectrum RX-IFTIR within wavenumber range of 4000-400 cm^{-1}. The X-ray diffraction was performed using RIGAKU Smart® lab 3kW X-ray Diffractometer from 20º to 80º Bragg's angle with step size 0.02 s with scan speed as 10º per min. The electron microscopic images were recorded using FEG-SEM and TEM; JEOL JSM-7600F FEG-SEM was used to obtain SEM images of sample, whereas JEOL, JEM-2100F was used for TEM analysis along with the SAED patterns. The HRTEM images were

recorded with accelerating voltage of 200 kV for high resolution imaging. The oxidation state of sample was deciphered using XPS analysis. Kratos Analytical Ltd AXIS Supra model X-ray photoelectron spectrophotmeter, equipped with a monochromatic Al Kα X-ray source at 1486.6 eV and a dual Al*K*α/Mg*K*α achromatic X-ray source was used for this purpose. The C 1s core level spectral peak was used for calibration. The sample was first etched with Ar^+ ion sputtering using Ar^+ ion at 500eV to clean the surface from surface oxidation and then analyzed using the aforementioned X-ray source.

RESULTS AND DISCUSSION

The purpose of this research was to produce Cu_2O nanoparticles embedded in a chitosan matrix. The blue colour of the reaction mixture due to copper sulphate pentahydrate taken as the metal precursor converted to pale blue and then finally, upon rise in pH to reddish brown with the formation of Cu_2O nanoparticles inside the polymer matrix [31]. The colour change observed is considered to be the preliminary indication of the formation of nanoparticles. Due to addition of dil. NaOH when the mixture was maintained at pH 8, the Cu_2O formed precipitates with chitosan present in the mixture as chitosan is insoluble in alkaline medium.

The Cu^{2+} ions when stirred with chitosan produce a light blue colour solution showing the complexation of Cu^{2+} ions due to the polar functional groups of chitosan matrix. The action of ethanol results in the reduction of Cu^{2+} to Cu^+ [23], in which pH plays important role [32]. Chitosan matrix acts as a stabilizer to control the growth of Cu_2O particles within nano-level, thus resulting in the formation of CS-Cu_2O nanocomposite [33].

UV-Visible absorbance studies: Fig. 1a shows the UV-visible spectrum of CS-Cu_2O nanocomposite recorded between 200 to 750 nm. A broad absorption peak for CS-Cu_2O nanocomposite was observed at 430 nm, corresponding to the surface plasmon resonance of the nanomaterial, which confirmed the formation of Cu_2O nanoparticles in the chitosan matrix. Another peak between 250-300 nm can be attributed to absorbance of the chitosan matrix in the ultraviolet region. The absorption in visible range is intense; also a steep gradient can be observed thus ruling out a transition due to impurity [34]. This peak position for Cu_2O nanoparticles has been reported by several other researchers also [35-39]. Tauc plot method was used to determine the band gap of the resulting nanoparticles and found to be 1.99 eV (Fig. 1b). The semiconducting nature of the prepared nanoparticles is thus confirmed through the aforementioned band gap analysis [40]. Thus, this nanocomposite can be potentially explored for its application in relevant fields. However, the slight lowering in the optical band gap than the reported band gap of 2.0-2.4 eV for Cu_2O is due to the chitosan coating. This lowering of band gap energy has been shown by other researchers as well for semiconducting metal oxide nanoparticles [4,41-43].

FTIR analysis: Fig. 2 represents the FTIR spectra of chitin, chitosan and chitosan-cuprous oxide (CS-Cu_2O) nanocomposite. In chitin (CH) spectra, the stretching vibrational frequencies related to C=O of the amide functional group can be observed by the two peaks at 1655 and 1621 cm^{-1}. The peak at 1655 cm^{-1} can be attributed to the stretching frequency of the C=O group which is linked to the N-H bond of neighbouring chain through hydrogen bonding, whereas, the another peak at 1621 cm^{-1} could be indicative of the amide C=O group hydrogen bonded to the OH group of the next chitin residue in the same chain. These peaks are also a clear indication for this chitin being an α-chitin. The peaks observed at 1310 cm^{-1} and 1552 cm^{-1} are assigned to amide C-N stretching vibrations and N-H bending vibrations of the amide, respectively. The peak at 1552 cm^{-1} verifies the structural conformation as being of the α-type. After deacetylation of chitin, the peak at 1552 cm^{-1} shifted to1562 cm^{-1} as shown in chitosan FTIR spectrum, confirmed the conversion of amide groups to amino groups [44-46].

A close observation of chitin and chitosan spectral data further verify the deacetylation of chitin to produce chitosan. The broad peak between 3500 and 3300 cm^{-1} is attributed to the newly formed $–NH_2$ groups, the peak of which have overlapped with the –OH groups and further developed hydrogen bonds with the water molecules existing in vicinity due to the

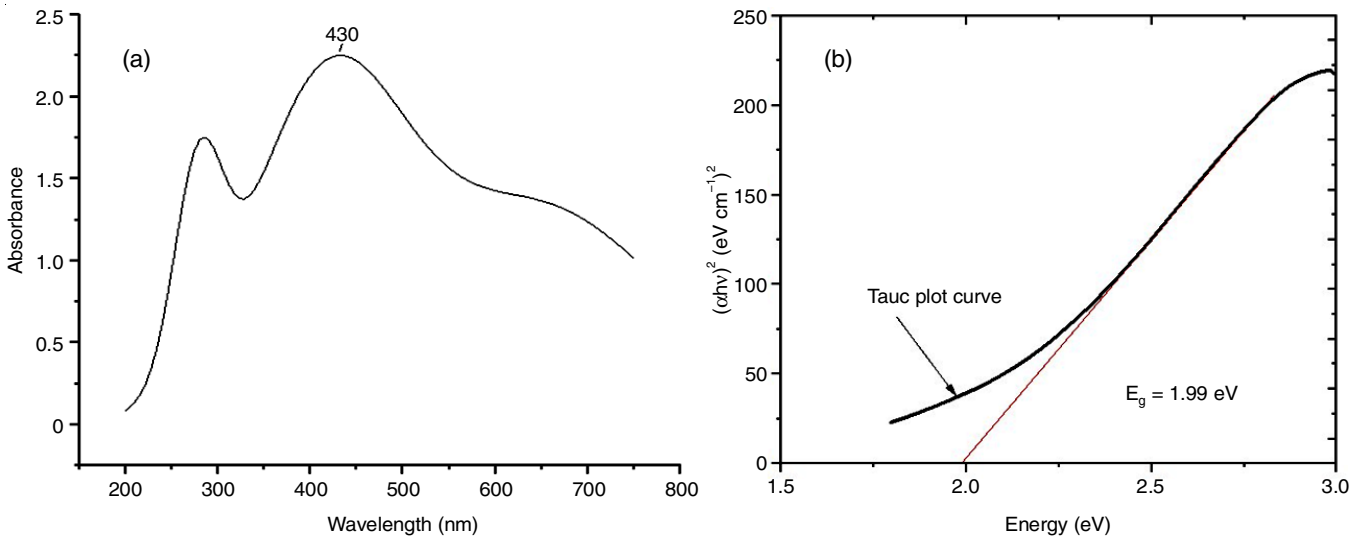

Fig. 1. (a) UV-Vis spectrum and (b) Tauc-plot of CS-Cu_2O nanocomposite

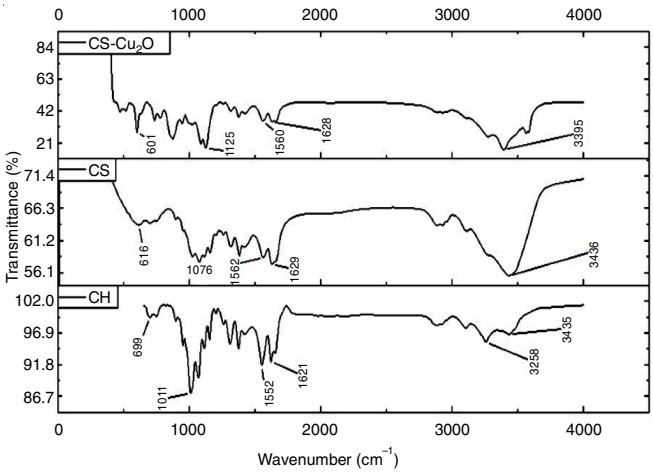

Fig. 2. FTIR spectra of chitin (CH), chitosan (CS) and CS-Cu_2O nanocomposite

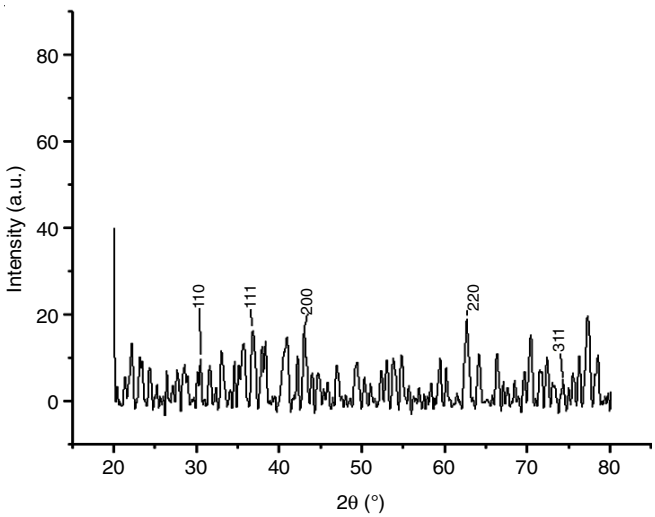

Fig. 3. XRD diffraction pattern of CS-Cu_2O nanocomposite

ambient moisture in air. This part of the spectrum further increases in intensity when CS-Cu_2O is formed, which suggests that the interaction of chitosan with Cu^{2+} has an important part to play in the formation of Cu_2O nanoparticles. The broad peak at 3436 cm^{-1} and the peak ~2800 cm^{-1} in chitosan, which is attributed to the well established stretching frequencies of –OH and $–NH_2$ groups, undergoes a red shift to 3395 cm^{-1}, indicating that these groups are involved in the complexation of Cu^{2+} to form CS-Cu_2O and keeps the newly formed nanoparticles stabilized [45]. A comparison of the intensities of the stretching frequency peaks in case of $–NH_2$ and in case of C=O of amide group shows that the amide groups in chitin have higher intensity than that of $–NH_2$, but the similar peaks in case of chitosan shows reverse pattern, *i.e.*, the broad peak for $–NH_2$ has stronger intensity than the peak for the carbonyl linkage of the amide group. This is a clear evidence of deacetylation of chitin to produce chitosan. A peak observed at 1629 cm^{-1} is associated with the C=O groups present in the biopolymer, which suggests that the deacetylation process undertaken to convert chitin into chitosan may be incomplete. This peak can also be observed at 1628 cm^{-1} in the FTIR spectrum of CS-Cu_2O nanocomposite. The degree of deacetylation (DD) can be calculated using the following formula [47]:

$$DD\ (\%) = 100 - \left(\frac{A_{1658}}{A_{3436}} \times 100 / 1.33 \right)$$

where A_{1658} and A_{3436} represent the absorbance values calculated from the obtained transmittance values at 1658 cm^{-1} and 3436 cm^{-1}, respectively. The degree of deacetylation was calculated to be 70%. The appearance of a sharp peak at 601 cm^{-1}, which is attributed to the formation of Cu_2O nanoparticles, is at a lower wavenumber than the usual 622 cm^{-1}, showing the stabilization of nanocomposite with chitosan [45].

XRD studies: Fig. 3 presents the XRD diffraction pattern of the chitosan-cuprous oxide (CS-Cu2O) nanocomposite, illustrating a characteristic nature of a polycrystalline material. Peaks at 2θ values 30.06º, 36.90º, 42.70º and 74.40º due to 110, 111 and 200 and 311 planes of Cu_2O were observed which were matched with JCPDS card no. 034-1354 indicating a cubic arrangement of Cu_2O in the synthesized nanocomposite [48-51]. The average crystallite size of the nanomaterial has been calculated using the famous Debye-Scherrer's equation:

$$D = \frac{k\lambda}{\beta \cos\theta}$$

where D represents the average crystallite size; λ is the wavelength of X-ray used (*i.e.* 1.54 Å); θ is the Bragg's angle; k denotes the shape related factor of 0.94 and β represents the full width at half maximum (FWHM) of the peak used.The calculated mean crystallite size was found to be 19.48 nm. The FWHM of sharp peak arising from the110 plane has been used as the numerical value of ß for this purpose [52]. Besides the peaks arising due to Cu_2O, the intense peak observd at 2θ value 20.20º shows the crystalline nature of chitosan and the observation of the aforementioned peaks confirmed the successful formation of the chitosan-Cu_2O nanocomposite [53,54].

Morphological studies: The image obtained through SEM (Fig. 4a) show the presence of spherical nanocomposite embedded in the chitosan matrix. The EDS spectrum (Fig. 4b) obtained during SEM analysis is consistent with the formation of CS-Cu_2O nanocomposite. The weight percentage for Cu as calcu-lated using the intensities depicted in the EDS plot is 25.86. The peak shown at 0.28 KeV represents carbon content, whereas those present at 0.4 KeV and 0.53 KeV are due to nitrogen and oxygen, respectively. The presence of C, N and O shown in the EDS analysis verify the other analyses supporting the stabilization of Cu_2O nanocomposite by chitosan and hence are considered as an evidence for the successful formation of CS-Cu_2O nanocomposite.

Fig. 5a-b shows HRTEM image of the sample recorded at 200 kV whereas Fig. 5c shows TEM image of the sample at 120 kV. Both of the imaging procedures revealed the presence of spherical Cu_2O nanoparticles. However, aggregates of those nanoparticles in the form of longitudinal structures can be seen, which further aggregate to form centrosymmetric nanostructures (Fig. 5b-c). This shows the crystalline nature of these nanoparticles resulting in their self-assembly into more complex nanostructures. A similar result has been reported using different reduction methods and for different metal nanoparticles [55,

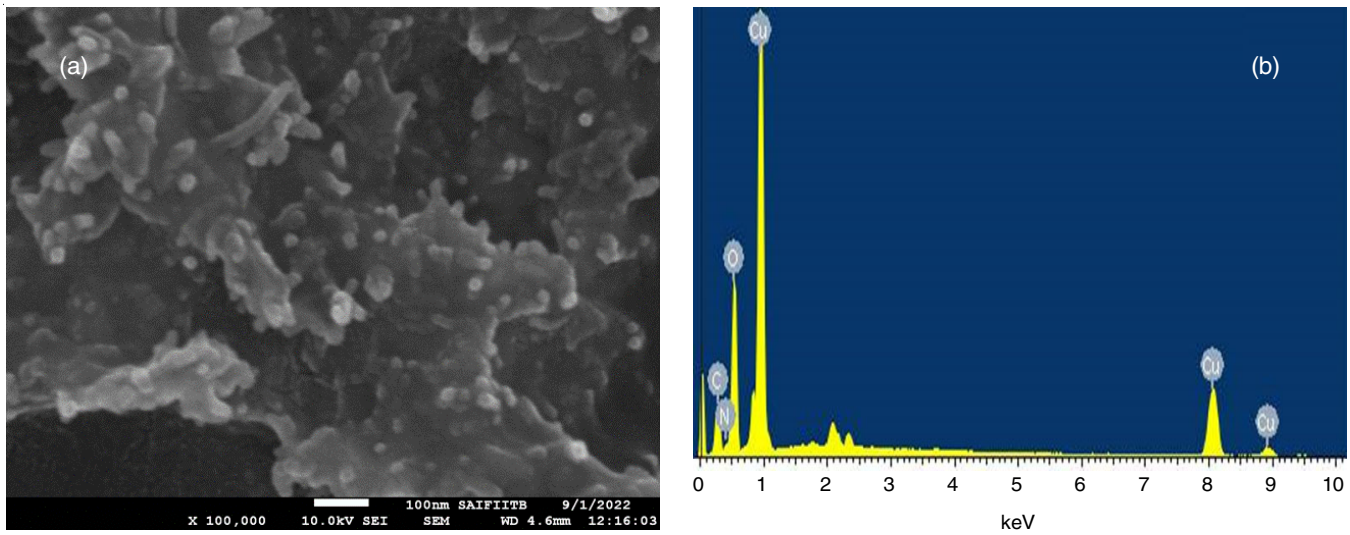

Fig. 4. (a) SEM image and (b) EDS spectra of CS-Cu_2O nanocomposite

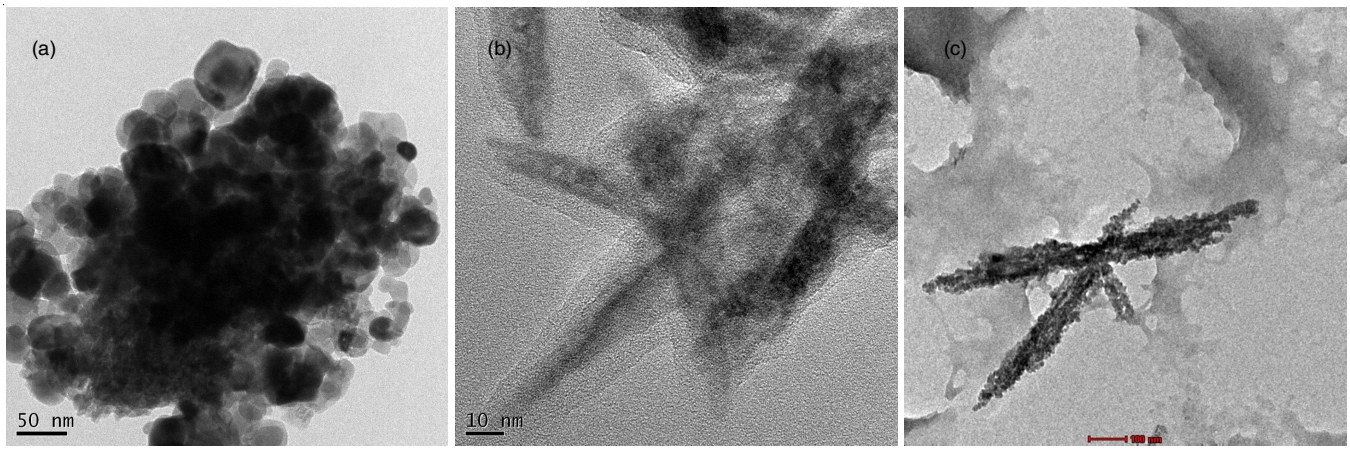

Fig. 5. TEM images of CS-Cu_2O nanocomposite

56]. However, this research has been successful in attaining the same using ethanol as a reducing agent.

The SAED pattern (Fig. 6) shows clear evidence of mutiphasic system with polycrystalline chitosan matrix along with crystalline Cu_2O nanoparticles. The measured d-spacing using diffraction due to 111 planes was found to be 0.269 nm.

XPS studies: The two major peaks in the XPS data as shown by the obtained plot (Fig. 7a) are Cu 2p3/2 and Cu 2p1/2 core-level peaks for copper. The binding energy of the Cu 2p3/2 core-level peak is 932 eV, while the binding energy of the Cu 2p1/2 core-level peak is 952.1 eV. The difference in binding energy between the two peaks is due to the different spin states of the electrons. The full width at half maximum value around 1.9eV also supports the formation of Cu^+ thus confirming Cu_2O [57]. The presence of these two major peaks in the XPS data suggests that the copper atoms in the nanocomposite are in a different chemical environment than metallic copper. This is due to copper atoms being stabilized by $–NH_2$ groups of chitosan, which has resulted in a shift in the binding energy of the Cu2p core-level peaks. Moreover, the presence of O 1s peak in the O1s spectra (Fig. 7b) at 530.9 eV confirms

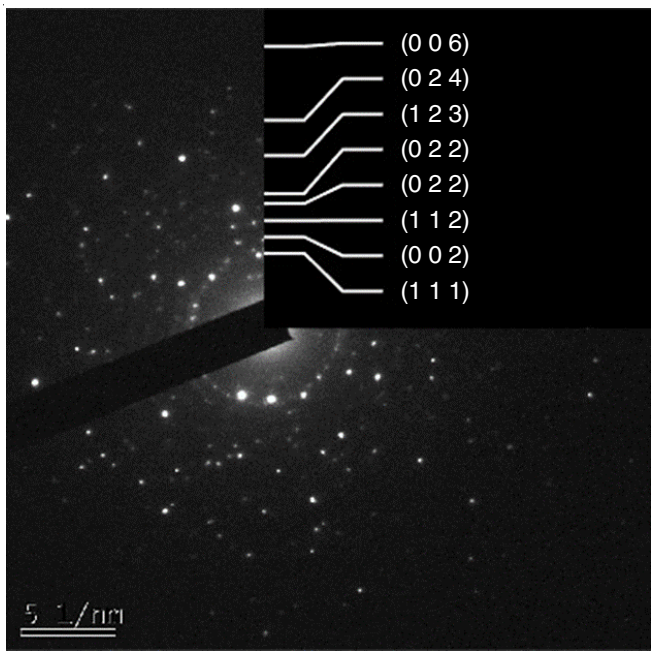

Fig. 6. SAED diffraction pattern of CS-Cu_2O nanocomposite

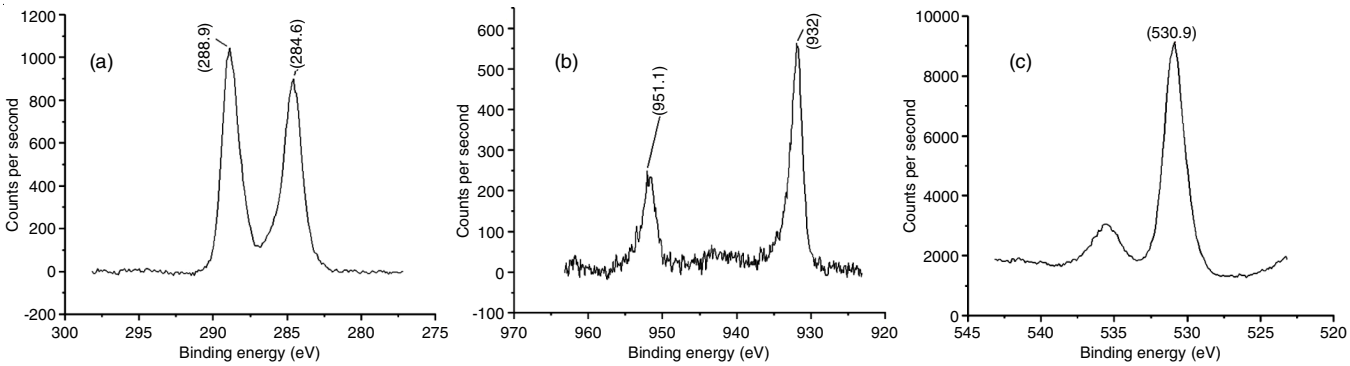

Fig. 7. XPS spectra of (a) C1s, (b) Cu2p and (c) O1s CS-Cu_2O nanocomposite

the formation of Cu_2O nanoparticles and ascribed to the Cu-O interaction [58]. This array of binding energies have been suggested by other researchers too as the evidence of Cu_2O nanoparticles [59,60].

Conclusion

The chitosan-Cu_2O nanocomposite was prepared using ethanol as reducing agent. In this work, the authors explored the ethanol based reduction of salt precursors for the synthesis of nanomaterials involving copper, especially to avoid harsh and toxic chemicals. The successful synthesis of the nanocomposite inside the polymeric matrix of chitosan was verified using sophisticated techniques such as SEM accompanied with EDS, TEM and SAED, FTIR, XRD and UV-visible analysis. The semiconductor nature of the chitosan embedded Cu_2O nanoparticles have been elucidated which can be of academic and research benefit.

CONFLICT OF INTEREST

The authors declare that there is no conflict of interests regarding the publication of this article.

REFERENCES

1. T.T.V. Phan, D.T. Phan, X.T. Cao, T.C. Huynh and J. Oh, *Nanomaterials*, **11**, 273 (2021); https://doi.org/10.3390/nano11020273
2. N. Baig, I. Kammakakam and W. Falath, *Mater. Adv.*, **2**, 1821 (2021); https://doi.org/10.1039/d0ma00807a
3. M. Rafique, A.J. Shaikh, R. Rasheed, M. Tahir, H.F. Bakhat, M. Rafique and F. Rabbani, *Nano*, **12**, 1750043 (2017); https://doi.org/10.1142/s1793292017500436
4. T.T.B. Quyen, N.N.T. My, D.T.T. Ngan, D.T. Pham and D.V.H. Thien, *Mongolian J. Chem.*, **22**, 31 (2021); https://doi.org/10.5564/mjc.v22i48.1564
5. N.A. Saad,, M.H. Dar, E. Ramya, S.R.G. Naraharisetty and D.N. Rao, *J. Mater. Sci.*, **54**, 188 (2018); https://doi.org/10.1007/s10853-018-2811-5
6. M. P. Nikolova and M.S. Chavali, *Biomimetics*, **5**, 27 (2020); https://doi.org/10.3390/biomimetics5020027
7. G. Borkow and J. Gabbay, *Curr. Chem. Biol.*, **3**, 272 (2009); https://doi.org/10.2174/187231309789054887
8. B. Sharma, P. Malik and P. Jain, *Mater. Today Commun.*, **16**, 353 (2018); https://doi.org/10.1016/j.mtcomm.2018.07.004
9. G.L. Vanti, S. Masaphy, M.M. Kurjogi, S.V. Chakrasali and V.B. Nargund, *Int. J. Biol. Macromol.*, **156**, 1387 (2020); https://doi.org/10.1016/j.ijbiomac.2019.11.179
10. A.Z. Hameed, S.A. Raj, J. Kandasamy, M.A. Baghdadi and M.A. Shahzad, *Polymers*, **14**, 2335 (2022); https://doi.org/10.3390/polym14122335
11. A. M. Muthukrishnan, *J. Nanomed. Nanotechnol.*, **6**, 251 (2015); https://doi.org/10.4172/2157-7439.1000251
12. M.M. Jaworska and G.A. Roberts, *Chem. Process Eng.*, **37**, 261 (2016); http://dx.doi.org/10.1515/cpe-2016-0021
13. C.P. Jiménez-Gómez and J.A. Cecili, *Molecules*, **25**, 3981 (2020); https://doi.org/10.3390/molecules25173981
14. B. Geng, Z. Jin, T. Li and X. Qi, *Sci. Total Environ.*, **407**, 4994 (2009); https://doi.org/10.1016/j.scitotenv.2009.05.051
15. E. Tabesh, H. Salimijazi, M. Kharaziha, M. Mahmoudi and M. Hejazi, *Surf. Coat. Technol.*, **364**, 239 (2019); https://doi.org/10.1016/j.surfcoat.2019.02.040
16. T. Jayaramudu, K. Varaprasad, R.D. Pyarasani, K.R. Reddy, K.D. Kumar, A. Akbari-Fakhrabadi, R.V. Mangalaraja and A. John, *Int. J. Biol. Macromol.*, **128**, 499 (2019); https://doi.org/10.1016/j.ijbiomac.2019.01.145
17. N. Ali, Awais, T. Kamal, M. Ul-Islam, A. Khan, S.A.A. Shah and A. Zada, *Int. J. Biol. Macromol.*, **111**, 832 (2018); https://doi.org/10.1016/j.ijbiomac.2018.01.092
18. N.M. Zain, A.G.F. Stapley and G. Shama, *Carbohydr. Polym.*, **112**, 195 (2014); https://doi.org/10.1016/j.carbpol.2014.05.081
19. M. Usman, N.A. Ibrahim, K. Shameli, N. Zainuddin and W.M.Z.W. Yunus, *Molecules*, **17**, 14928 (2012); https://doi.org/10.3390/molecules171214928
20. K. Tokarek, J.L. Hueso, P. Kustrowski, G. Stochel and A. Kyziol, *Eur. J. Inorg. Chem.*, **2013**, 4940 (2013); https://doi.org/10.1002/ejic.201300594
21. E. M. Bakhsh, F. Ali, S. B. Khan, H. M. Marwani, E. Y. Danish, A. M. Asiri, *Int. J. Biol. Macromol.*, **131**, 666 (2019); https://doi.org/10.1016/j.ijbiomac.2019.03.095
22. S. Chandra, A. Kumar and P.K. Tomar, *J. Saudi Chem. Soc.*, **18**, 149 (2014); https://doi.org/10.1016/j.jscs.2011.06.009
23. A. Pal, S. Shah and S. Devi, *Mater. Chem. Phys.*, **114**, 530 (2009); https://doi.org/10.1016/j.matchemphys.2008.11.056
24. M.C. Crisan, M. Teodora and M. Lucian, *Appl. Sci.*, **12**, 141 (2021); https://doi.org/10.3390/app12010141
25. J. Quinson, S. Neumann, L. Kacenauskaite, J.J.K. Kirkensgaard, J. Bucher, S.B. Simonsen, L.T. Kuhn, A. Zana, T. Vosch, M. Oezaslan, S. Kunz and M. Arenz, *Chem. Eur. J.*, **26**, 9012 (2020); https://doi.org/10.1002/chem.202001553
26. M. Prause, H. Schulz and D. Wagler, *Acta Biotechnol.*, **4**, 143 (1984); https://doi.org/10.1002/abio.370040210
27. M.B. Kumar, *React. Funct. Polym.*, **46**, 1 (2000); https://doi.org/10.1016/s1381-5148(00)00038-9
28. H.E. Knidri, R. Belaabed, A. Addaou, A. Laajeb and A. Lahsini, *Int. J. Biol. Macromol.*, **120**, 1181 (2018); https://doi.org/10.1016/j.ijbiomac.2018.08.139
29. S. Ayyappan, R. Gopalan, G. N. Subbanna and C.N.R. Rao, *J. Mater. Res.*, **12**, 398 (1997); https://doi.org/10.1557/jmr.1997.0057
30. H.J. Hah, S.M. Koo and S.H. Lee, *J. Sol-Gel Sci. Technol.*, **26**, 467 (2003); https://doi.org/10.1023/A:1020710307359

31. B. Kodasi, R.R. Kamble, J. Manjanna, S.R. Hoolageri, L. Bheemayya, V.B. Nadoni, P.K. Bayannavar, S. Dixit, S.K. Vootla and V.M. Kumbar, *J. Trace Elem. Miner.*, **3**, 100044 (2023); https://doi.org/10.1016/j.jtemin.2022.100044
32. N. Zayyoun, L. Bahmad, L. Laânab and B. Jaber, *Appl. Phys. A*, **122**, 488 (2016); https://doi.org/10.1007/s00339-016-0024-9
33. D. Verma, R. Malik, J. Meena and R. Rameshwari, *J. Appl. Nat. Sci.*, **13**, 544 (2021); https://doi.org/10.31018/jans.v13i2.2635
34. Y. Wang, L. Chen, H. Yang, Q. Guo, W. Zhou and M. Tao, *Mater. Sci. Poland*, **28**, 467 (2010).
35. S. M. Butte and S. A. Waghuley, *AIP Conf. Proc.*, **2220**, 020093 (2020); https://doi.org/10.1063/5.0001644
36. S.S. Sawant, A.D. Bhagwat and C.M. Mahajan, *J. Nano-Electron. Phys.*, **8**, 01035 (2016); https://essuir.sumdu.edu.ua/handle/123456789/44869
37. A. Rezaie, M. Montazer and M.M. Rad, *Fibers Polym.*, **18**, 1269 (2017); https://doi.org/10.1007/s12221-017-7263-z
38. J.M. Prajapati, D. Das, S. Katlakunta, N. Maramu, V. Ranjan and S. Mallick, *Inorg. Chim. Acta*, **515**, 120069 (2021); https://doi.org/10.1016/j.ica.2020.120069
39. A. Yang, S.-P. Li, Y. Wang, L. Y. Wang, X. Bao and R. Yang, *Trans. Nonferrous Met. Soc. China*, **25**, 3643 (2015); https://doi.org/10.1016/s1003-6326(15)64005-5
40. A. Oral, E. Mensur, M. Aslan, E. Basaran, *Mater. Chem. Phys.*, **83**, 140 (2004); https://doi.org/10.1016/j.matchemphys.2003.09.015
41. J. Shu, Z. Wang, Y. Huang, N. Huang, C. Ren and W. Zhang, *J. Alloys Compds.*, **633**, 338 (2015); https://doi.org/10.1016/j.jallcom.2015.02.048
42. T.U. Rahman, H. Roy, A.Z. Shoronika, A. Fariha, M. Hasan, M.S. Islam, H.M. Marwani, A. Islam, M.M. Hasan, A.K. Alsukaibi, M.M. Rahman and M.R. Awual, *J. Mol. Liq.*, **388**, 122764 (2023); https://doi.org/10.1016/j.molliq.2023.122764
43. B.A. Koiki and O.A. Arotiba, *RSC Adv.*, **10**, 36514 (2020); https://doi.org/10.1039/d0ra06858f
44. E. M. Dahmane, M. Taourirte, N. Eladlani and M. Rhazi, *Int. J. Polym. Anal. Characteriz.*, **19**, 342 (2014); https://doi.org/10.1080/1023666x.2014.902577
45. J. Chen, P. Zhou, J.-L. Li and S. Li, *Carbohydr. Polym.*, **67**, 623 (2007); https://doi.org/10.1016/j.carbpol.2006.07.003
46. M. Rinaudo, *Progr. Polym. Sci.*, **31**, 603 (2006); https://doi.org/10.1016/j.progpolymsci.2006.06.001
47. B. Fatima, eds.: M. Khan, G.M. do Nascimento and M. El-Azazy, Quantitative Analysis by IR: Determination of Chitin/Chitosan DD, In: Modern Spectroscopic Techniques and Applications, IntechOpen eBooks (2020); https://doi.org/10.5772/intechopen.89708
48. J. Wang, W. Xiao, H. Teng, H.-M. Yin, X. Chen, J. Xianjing, C. Huo, M. Teng, S. Ma and A.A.N.M. Al-Haimi, *Environ. Technol.*, **41**, 2157 (2020); https://doi.org/10.1080/09593330.2018.1556740
49. Z. Li, Y. Zhang, H. Yu and H. Zhao, *Ceram. Int.*, **48**, 4066 (2022); https://doi.org/10.1016/j.ceramint.2021.10.196
50. A. El-Shaer, W. Ismail and M. Abdelfatah, *Mater. Res. Bull.*, **116**, 111 (2019); https://doi.org/10.1016/j.materresbull.2019.04.005
51. S. Kapoor, N. Goel and S. Singhal, *Mater. Today: Proc.* **14(Part 2)**, 445 (2019); https://doi.org/10.1016/j.matpr.2019.04.167
52. H. Lahmar, F. Setifi, A. Azizi, G. Schmerber and A. Dinia, *J. Alloys Compds.*, **718**, 36 (2017); https://doi.org/10.1016/j.jallcom.2017.05.054
53. Y. Xu, K.M. Kim, M.A. Hanna and D. Nag, *Ind. Crops Prod.*, **21**, 185 (2005); https://doi.org/10.1016/j.indcrop.2004.03.002
54. M. Kaya, T. Baran, A. Mentes, M. Asaroglu, G. Sezen and K.Ö. Tozak, *Food Biophys.*, **9**, 145 (2014); https://doi.org/10.1007/s11483-013-9327-y
55. T.T.V. Phan, G. Hoang, V.T. Nguyen, T.P. Nguyen, H.H. Kim, S. Mondal, P. Manivasagan, M.S. Moorthy, K.D. Lee and O. Junghwan, *Carbohydr. Polym.*, **205**, 340 (2019); https://doi.org/10.1016/j.carbpol.2018.10.062
56. L. Chen, Y. Zhang, R. Sun, F. Zhou, W. Zeng, D. Lu and C.-P. Wong, *Sci. Rep.*, **5**, 9672 (2015); https://doi.org/10.1038/srep09672
57. T. Abiraman and S. Balasubramanian, *Ind. Eng. Chem. Res.*, **56**, 1498 (2017); https://doi.org/10.1021/acs.iecr.6b04692
58. M. Sportelli, A. Volpe, R. Picca, A. Trapani, C. Palazzo, A. Ancona, P. Lugarà, G. Trapani and N. Cioffi, *Nanomaterials*, **7**, 6 (2017); https://doi.org/10.3390/nano7010006
59. P.V.F. De Sousa, A.F. De Oliveira, A.A. Da Silva and R.P. Lopes, *Environ. Sci. Pollut. Res. Int.*, **26**, 14883 (2019); https://doi.org/10.1007/s11356-019-04989-3
60. M. Kumar, V. Bhatt, O.S. Nayal, S. Sharma, V. Kumar, M.S. Thakur, N. Kumar, R. Bal, B. Singh and U. Sharma, *Catal. Sci. Technol.*, **7**, 2857 (2017); https://doi.org/10.1039/c7cy00832e